JMEPEG (2010) 19:90–98
DOI: 10.1007/s11665-009-9416-8

1059-9495/$19.00

An Experimental Study of the Corrosion Behavior of Nickel Tungsten Carbide in Some Water-Glycol Hydraulic Fluids for Subsea Applications

Lei Zheng, Anne Neville, Andrew Gledhill, and David Johnston

(Submitted August 18, 2008; in revised form February 17, 2009)

Corrosion failures of components in electro-hydraulic control systems can have serious consequences for the operation of an entire subsea oil recovery system, especially in water depths more than 150 m (Fleming, *Meas. Control*, 2000, 33(7), p 207–213). An acceptable reason for this is that seawater ingress can have a great effect on stainless steel 316L, the most commonly used material for the failed components of the direction control valves, since chloride irons destabilize the passive film [Malik et al., *Corros. Sci.*, 1992, 33(11), p 1809–1827; *Desalination*, 1994, 97(1–3), p 189–197; Al-Malahy and Hodgkiess, *Desalination*, 2003, 158(1–3), p 35–42]. Other materials, claimed to be seawater tolerant, are starting to be used in this system. However, problems can still exist due to the complex factors relating to the corrosion process and how the environmental parameters affect the corrosion mechanisms. In this work, the corrosion behavior of a nickel tungsten carbide cermet, one of the proposed materials, is compared with stainless steel 316L, in four different water-glycol hydraulic fluids and 50% hydraulic fluid/50% seawater solutions using an electrochemical test methodology. Systematic fluid analysis, which includes GC-MS for organic components and ICP-MS analysis for ionic content, and surface analysis of the material are carried out to assess the corrosion mechanisms. Detailed conclusions are then made to summarize the advantages and disadvantages of nickel tungsten carbide being used in this system. The effects of each factor on the corrosion rates and mechanisms are discussed.

Keywords corrosion, hydraulic fluids, nickel tungsten carbide, stainless steel 316L

1. Introduction

1.1 Industry Problem and Study Objectives

The serious consequences of corrosion remain a problem in the offshore industry, with its complex and demanding production techniques, and the environmental threat should components fail leading to hydrocarbon leaks. Technological advances have allowed people to venture into deeper and deeper water for oil and gas. The direction control valves (DCVs) are referred to as the most susceptible components to corrosion in an open loop hydraulic system that controls subsea operations, particularly the pilot-stage valve spindles and the balls that allow the flow of hydraulic fluid when it is displaced from its seat (Ref 1) according to BP's experience.

In February 1999, the Schiehallion Oilfield, located 150 km West of Shetland, was shutdown only 7 months after production began. The failed subsea control system was an E/H multiplexed system of open hydraulic configuration utilizing water-glycol hydraulic fluid and the main parts said to be responsible were the DCVs fabricated from stainless steel 316L. Subsequent investigation concluded that the primary damage was associated with seawater ingress that may degrade the fluid and is very corrosive to stainless steel 316L (Ref 2-4). Figure 1 shows the DCV and the key components blamed for failure are enlarged.

Significant efforts were made to minimize the risk of seawater ingress during initial equipment installation; however, it was really difficult to avoid in long-term running. Consequently, actions have been taken to identify and qualify DCV pilot-stage materials more tolerant to the effects of seawater contamination of the fluids being used in the hydraulic system.

In this work, the performance of nickel tungsten carbide, one of the proposed materials (Ref 5), was investigated in conditions simulating the operating environment. A comparison with stainless steel 316L is made based on the results of electrochemical tests in four commonly used water-glycol hydraulic fluids. The corrosivity to nickel tungsten carbide was also ranked. The effects of seawater ingress and temperature were assessed. Systemic chemical analysis of each fluid was carried out to enable links to the corrosion mechanisms of the active components to be made.

1.2 Water-Glycol Hydraulic Fluids

Water-glycol solutions (HFC) are one of the most commonly used hydraulic fluids in applications where fire hazard is a concern such as in the offshore oil industry (Ref 6). They contain from 35 to 60% water to provide fire resistance, plus a glycol antifreeze such as ethylene, diethylene, or propylene which is

Lei Zheng and **Anne Neville**, Institute of Engineering Thermofluids, Surfaces and Interfaces, School of Mechanical Engineering, University of Leeds, Woodhouse Lane, Leeds LS2 9JT, UK; and **Andrew Gledhill** and **David Johnston**, Aker-Kvaerner Subsea Ltd, Howe Moss Avenue, Kirkhill Industrial Estate, Dyce, Aberdeen AB21 0NA, Scotland, UK. Contact e-mail: menlz@leeds.ac.uk.

non-toxic and biodegradable, and a thickener such as polyglycol to provide the required viscosity (Ref 7). These fluids also comprise other important additives such as sodium sulphonates, fatty acid esters, esters of phosphoric acid, amine salts, carboxylic acids, and acid esters up to 10% (Ref 8) to provide protection against wear, foam, corrosion, and microbiological degradation. Fluorescent dyes are added as well for leak detection. The fluids are compatible with conventional nitrile rubber, but are extremely aggressive to many types of paint coating (Ref 9).

In this study, four fluids are involved, supplied by two different manufacturers: HW525 and HW540 from Macdermid Offshore and HT and HT2 from Castrol Offshore. HW525 is a blue fluid with 25% glycol content, while HW540 has more glycol (up to 40%) and is darker. The additive packages in these two fluids are the same and both of them contain molybdenum disulphide (Ref 1). HT and HT2 also have similar components to each other. The only difference is that they use different dyes for leaking track purpose. The ethylene glycol contents are also the same.

1.3 Materials Under Study

Nickel tungsten carbide is a metal matrix composite where tungsten carbide particles are the aggregate and metallic nickel serves as the matrix. The nickel binder gives this material relatively high corrosion resistance and it is supposed to be seawater tolerant. In this study, the nickel tungsten carbide sample is directly cut from a DCV and analyzed by SEM/EDX before the test. In Fig. 2, the surface microstructure is shown alongside the elemental composition. It has about 6.3 wt.% nickel and the hard phase is apparently a Monotungsten Carbide and Tungsten Dicarbide mixture.

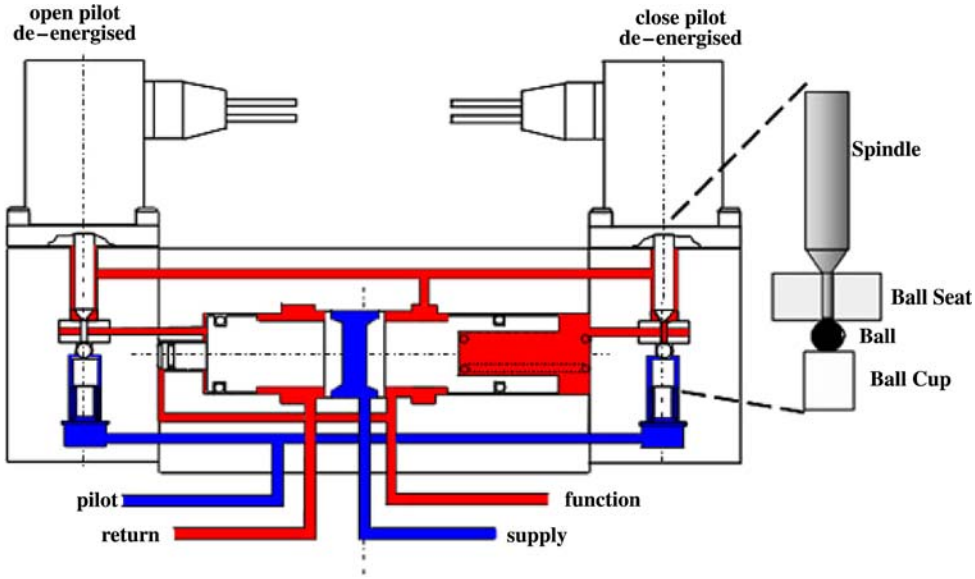

Fig. 1 A schematic diagram of the directional control valve

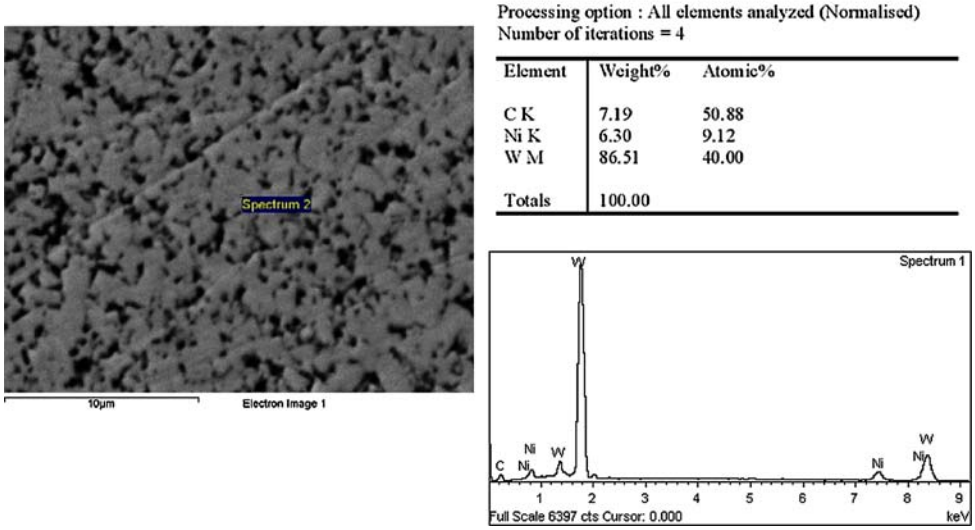

Fig. 2 SEM/EDX analysis of received nickel tungsten carbide sample

Stainless steel 316L (UNS S31603) is an extra-low carbon version of type 316. It has good corrosion resistance due to the presence of an adherent passive film, where chromium forms an oxide which then passivates the material (Ref 10). It is usually regarded as the standard "marine grade stainless steel"; however, it is not resistant to warm seawater where pitting and crevice corrosion can be prevalent.

2. Experimental Methods

2.1 Cyclic Potentiodynamic Polarization

The cyclic potentiodynamic polarization test (CPP) method makes use of a three-electrode electrochemical cell and plots a forward and reverse scan. The reference electrode used in all experiments is silver/saturated-silver-chloride half cell, the potential of which versus normal hydrogen electrode (NHE) is +0.197 V. The working electrode is the sample and platinum is used as the counter electrode. The potential is controlled by a computer-controlled potentiostat (EG&G) and is shifted at a constant rate in the anodic direction from the open circuit potential (OCP), causing the working electrode to become the anode and causing electrons to be withdrawn from it at first. After the current density reaches a value of 500 $\mu A/cm^2$, the potential then drops step by step to return to the OCP. The scan rate is set to 0.25 mV/s.

Experimental samples were prepared in a way that only a known surface area of 100 mm^2 was exposed. Setting the sample into resin accomplished this. A wire was initially soldered to the sample and this was placed in a mould so that resin totally surrounded the sample and bare metal of the wire. The exposed area was polished using 240, 600, and 1200 grit silicon carbide paper to a mirror finish and was rinsed with distilled water and dried carefully with compressed air before electrochemical test.

Artificial seawater (pH 8.24, 3.5% salinity, 54 mS/cm conductivity, the composition shown in Table 1) was prepared using distilled water and sea salt to simulate seawater ingress.

2.2 Gas Chromatography-Mass Spectrometry

Gas chromatography-mass spectroscopy (GC-MS) is one of the so-called hyphenated analytical techniques. As the name implies, it is actually two techniques that are combined to form a single method of analyzing mixtures of chemicals.

Gas chromatography is used to separate mixtures of chemicals into individual components. Each compound elutes from the column and enters a detector at a different rate, which depends on the molecule size, the adhesive force between the compound and the column, and the chemical properties of it.

Table 1 Composition of artificial seawater

Ion	Average, g/kg Salinity = 3.5%
Chloride (Cl^-)	19.353
Sodium (Na^+)	10.760
Sulphate (SO_4^-)	2.712
Magnesium (Mg^{2+})	1.297
Calcium (Ca^{2+})	0.412
Potassium (K^+)	0.399

Each of the peaks in the chromatogram represents the signal created when a compound enters the detector.

As the individual compounds elute from the GC column, they enter the electron ionization (mass spectrometer) detector to be identified. The mass spectrometer does this by breaking each molecule into ionized fragments and detecting these fragments using their mass to charge ratio (M/Z). Each molecule has a specific fragment spectrum which allows for its determination.

In this study, all four fluids were extracted into dichloromethane (DCM) before analysis to remove the glycol contents so that they do not dominate the chromatogram. Due to the limitation of this technique, the exact components of each fluid cannot be obtained.

2.3 Inductively Coupled Plasma Mass Spectrometry

Inductively coupled plasma mass spectrometry (ICP-MS) is highly sensitive and capable of analysis of a range of metals and several non-metals at below one part in 10^{12}. It is based on coupling together an inductively coupled plasma as a method of producing ions (ionization) with a mass spectrometer as a method of identifying and detecting the ions. The concentration of a sample can be determined through calibration with elemental standards.

In this study, ICP-MS was used to trace the metal ions before and after the corrosion process. The fluid samples were digested in nitric acid before analysis.

3. Results and Discussion

3.1 Comparing the Corrosion Behavior of Nickel Tungsten Carbide with Stainless Steel 316L in Pure HW525

Figure 3 was generated from the CPP test data in pure HW525 at 20 °C. It is clear that stainless steel 316L performs better than nickel tungsten carbide under this condition. This can be inferred from four aspects:

- Stainless steel 316L has a passive range on the forward scan. The current density does not increase until the potential arrives at a specific value, which is so-called "breakdown" potential (E_b). Nickel tungsten carbide does not exhibit passivity but displays active corrosion behavior such that Tafel extrapolation can be made to calculate the corrosion current density (i_{corr}). The current density keeps increasing from the OCP with the potential step by step.
- The i_{corr} value of nickel tungsten carbide under this condition is 1.51 $\mu A/cm^2$, whereas for stainless steel 316L is 1 $\mu A/cm^2$. However, the value is difficult to determine with precision since the current are low and the material does not exhibit activation controlled corrosion. Quoting i_{corr} values for passive materials can often be misleading.
- The reverse potential (E_r) of stainless steel 316L is much higher than that of nickel tungsten carbide. It is the potential at which the current density reaches 500 $\mu A/cm^2$. It demonstrates that a much larger over-potential is required for corrosion propagation on stainless steel 316L and hence it can be said to have better resistance under these conditions.
- Both curves have a negative hysteresis. The current density decreases when the potential drops on the reverse scan. In this case, the current density drops faster than it

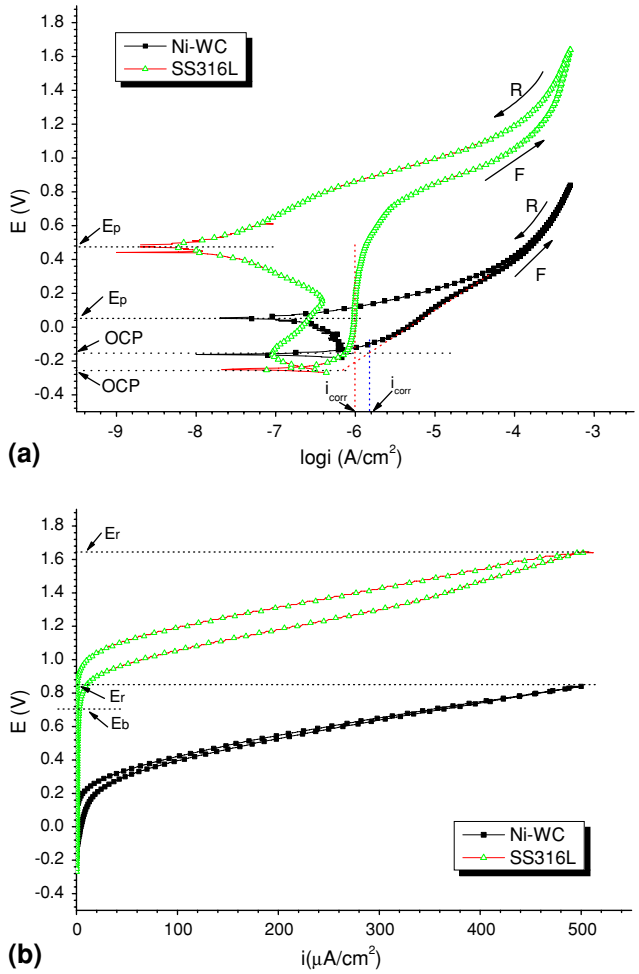

Fig. 3 CPP curves of nickel tungsten carbide and stainless steel 316L in HW525 at 20 °C. F, forward scan; R, reverse scan. (a) (E vs. log i); (b) (E vs. i)

increases on the forward scan (the reverse scan branch is above the forward one). A protection potential (E_p) appears on the reverse scan, below which the test sample will become cathode. The protection potential of stainless steel 316L is higher than that of nickel tungsten carbide as well. For a material which shows passive behavior (as stainless steel 316L in this case), it is also referred to as a repassivation potential.

The same tests were carried out at 50 and 70 °C. From Fig. 4 and 5, the following information can be obtained:

- At high temperature, the corrosion process for both materials is accelerated as expected. The E_r and E_p values of both materials decrease and the i_{corr} value increases. The breakdown also occurs at a lower (more active) potential for stainless steel 316L.
- The reverse scan of stainless steel 316L was notably affected by temperature. The E_p value drops much faster than that of nickel tungsten carbide with increased temperature. Furthermore, the trend of the curve changes at 70 °C. The reverse scan branch intersects the forward scan since the current density decreases slower than the increase rate on the forward scan after that point.

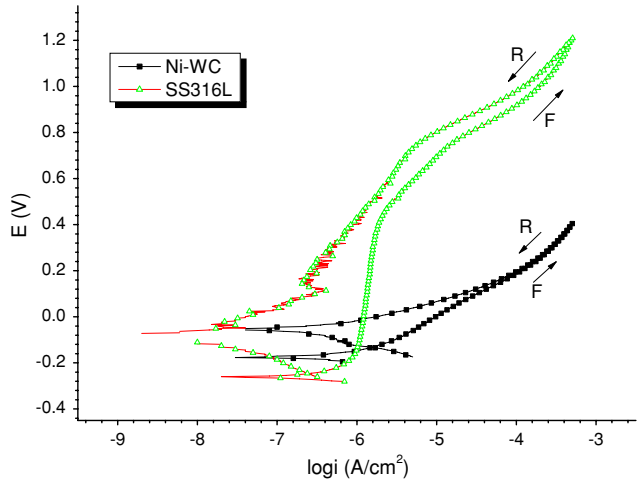

Fig. 4 CPP curves (E vs. log i) of nickel tungsten carbide and stainless steel 316L in HW525 at 50 °C

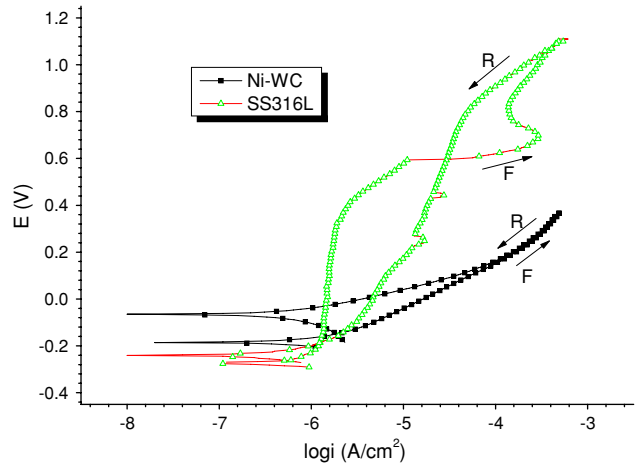

Fig. 5 CPP curves (E vs. log i) of nickel tungsten carbide and stainless steel 316L in HW525 at 70 °C

From the electrochemical results, it can be said that nickel tungsten carbide performs in a more stable manner than stainless steel 316L at higher temperature (50 °C/70 °C). The two materials corrode by different mechanisms. Stainless steel 316L is corroded when local breakdown of the passive film occurs and the nickel tungsten carbide corrodes in a more general manner (as will be discussed later), although on a micro scale there are some local variations. Increasing temperature affects the kinetics of the corrosion process but does not appear to change the corrosion mechanisms (localized or general). On stainless steel 316L, corrosion initiates and propagates pits. At lower temperature, these small pits can repair themselves after breakdown and the curve shows a negative hysteresis. However, at high temperature, the breakdown potential is lowered (lower E_b) but more dramatically the pits are stabilized as demonstrated by a large hysteresis and the repassivation process becomes more difficult. For Ni-WC the corrosion current density progressively increases as the temperature increases in an almost linear manner.

A detailed comparison of the electrochemical parameters for these two materials in pure HW525 is presented in Table 2.

Table 2 Comparison of nickel tungsten carbide with stainless steel 316L in pure HW525 at different temperatures (20, 50, and 70 °C)

	20 °C		50 °C		70 °C	
	Ni-WC	SS316L	Ni-WC	SS316L	Ni-WC	SS316L
E_b, V	N/A	0.62	N/A	0.55	N/A	0.45
E_r, V	0.85	1.64	0.41	1.22	0.37	1.11
E_p, V	0.05	0.47	−0.06	−0.06	−0.07	−0.24
OCP, V	−0.15	−0.25	−0.17	−0.26	−0.18	−0.27
i_{corr}, μA/cm^2	1.51	1.01	1.74	1.26	2.14	1.45

Table 3 Comparison of nickel tungsten carbide with stainless steel 316L in pure HW540 at different temperatures (20, 50, and 70 °C)

	20 °C		50 °C		70 °C	
	Ni-WC	SS316L	Ni-WC	SS316L	Ni-WC	SS316L
E_b, V	N/A	0.56	N/A	0.45	N/A	0.38
E_r, V	0.89	1.67	0.64	1.65	0.43	1.31
E_p, V	−0.10	0.16	−0.11	0.02	−0.12	0.06
OCP, V	−0.18	−0.33	−0.20	−0.34	−0.20	−0.36
i_{corr}, μA/cm^2	1.87	1.48	1.91	2.18	1.99	1.77

Table 4 Comparison of nickel tungsten carbide with stainless steel 316L in pure HT at different temperatures (20, 50, and 70 °C)

	20 °C		50 °C		70 °C	
	Ni-WC	SS316L	Ni-WC	SS316L	Ni-WC	SS316L
E_b, V	N/A	0.74	N/A	0.65	N/A	0.58
E_r, V	0.70	1.27	0.40	1.18	0.22	1.09
E_p, V	−0.12	0.59	−0.14	0.37	−0.18	0.26
OCP, V	−0.19	−0.32	−0.21	−0.33	−0.23	−0.34
i_{corr}, μA/cm^2	2.83	1.04	4.68	1.23	5.25	1.26

Table 5 Comparison of nickel tungsten carbide with stainless steel 316L in pure HT2 at different temperatures (20, 50, and 70 °C)

	20 °C		50 °C		70 °C	
	Ni-WC	SS316L	Ni-WC	SS316L	Ni-WC	SS316L
E_b, V	N/A	0.72	N/A	0.61	N/A	0.57
E_r, V	1.04	1.30	0.41	1.18	0.31	1.11
E_p, V	−0.10	0.64	−0.17	0.45	−0.19	0.36
OCP, V	−0.21	−0.30	−0.22	−0.31	−0.24	−0.32
i_{corr}, μA/cm^2	2.40	1.01	3.80	1.18	5.37	1.20

In the other three fluids, the results are quite similar. The electrochemical results are presented in Table 3-5 accordingly.

3.2 Comparing the Corrosion Behavior of Nickel Tungsten Carbide with Stainless Steel 316L in 50% HW525-50% Seawater at 50 °C

Figure 6 and Table 6 indicate that seawater ingress is extremely detrimental to stainless steel 316L. Nickel tungsten carbide is significantly more tolerant to this.

The following key observations are made in relation to seawater ingress.

- Seawater ingress greatly decreases E_b, E_r, E_p, and OCP values of stainless steel 316L. The effect on nickel tungsten carbide is to increase i_{corr}.
- When mixed with seawater, the conductivity of this solution is higher than pure HW525 and the concentration of Cl^- ions is increased. These factors accelerate the corrosion process of nickel tungsten carbide, but it does not

change the general trend of the curve. However, the curve of stainless steel 316L now has a positive hysteresis. This material cannot repair itself after breakdown and the current density increases even when the potential drops. Pits will propagate and serious localized corrosion occurs in this chloride-ion environment. This pitting corrosion phenomenon and the detrimental effect of Cl^- have been described many times in the literature (Ref 11-13).

Figure 7 presents the totally different surface condition of these two materials after the test in 50% HW525-50% seawater.

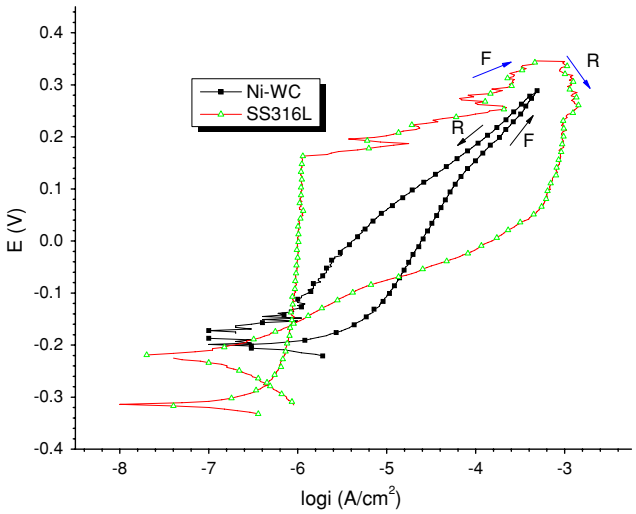

Fig. 6 CPP curves (E vs. log i) of nickel tungsten carbide and stainless steel 316L in 50% HW525-50% seawater at 50 °C

Table 6 Comparison of nickel tungsten carbide with stainless steel 316L in 50% HW525-50% seawater at 50 °C

	Ni-WC		SS316L	
Seawater content	**None**	**50%**	**None**	**50%**
E_b, V	N/A	N/A	0.55	0.16
E_r, V	0.41	0.29	1.22	0.35
E_p, V	−0.06	−0.06	−0.06	−0.24
OCP, V	−0.17	−0.19	−0.26	−0.31
i_{corr}, μA/cm^2	1.74	4.67	1.26	1.00

3.3 Comparing the Corrosion Behavior of Nickel Tungsten Carbide in Four Different Pure Fluids at 50 °C

Not unexpectedly, in addition to temperature, seawater ingress and the material itself, different components in the fluids also have an effect on the corrosion process. CPP curves of nickel tungsten carbide in the four fluids (HT, HT2, HW525, and HW540) at 50 °C are compared in Fig. 8.

The general form of the curves is the same. HW540 is least corrosive to nickel tungsten carbide. The rate of increase of current density as a function of potential in HW540 is smaller than in all other fluids and the reverse potential is the highest. The corrosion current density is the lowest. All the relevant CPP parameters are presented in Table 7.

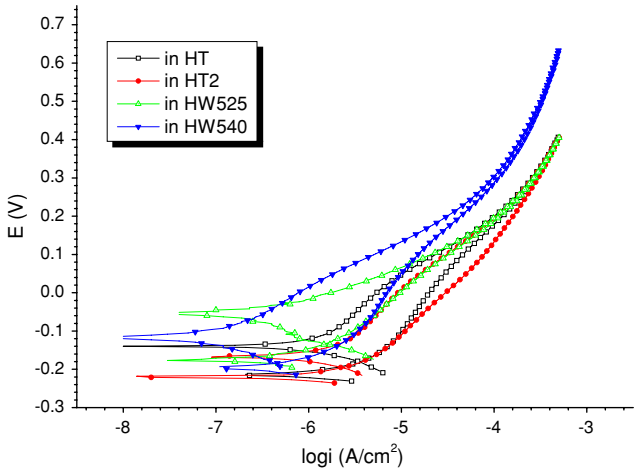

Fig. 8 CPP curves (E vs. log i) of nickel tungsten carbide in four fluids at 50 °C

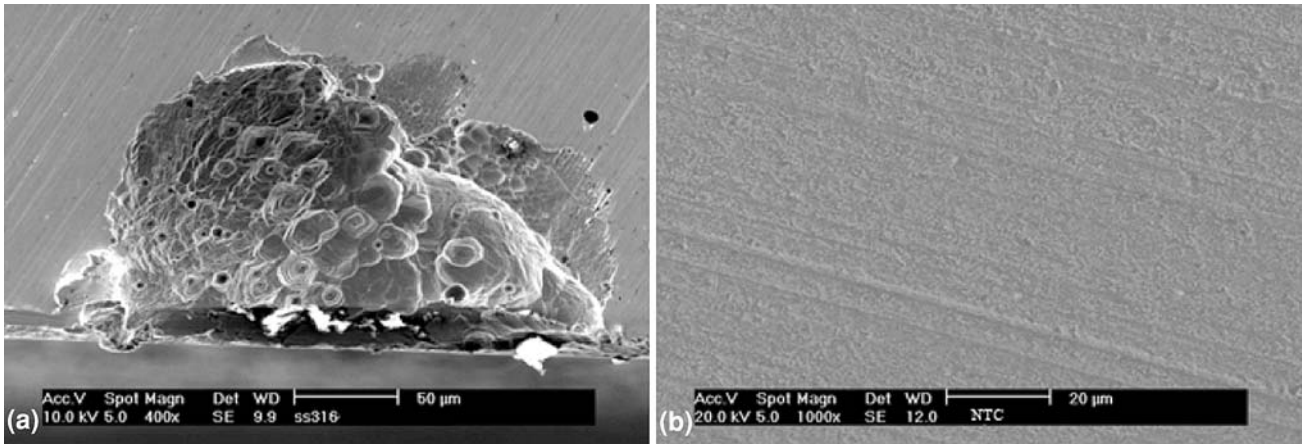

Fig. 7 SEM images of stainless steel 316L (a) and nickel tungsten carbide (b) after test in 50% HW525-50% seawater at 50 °C

Following chemical analysis of the fluids there is information of the key constitution of the fluids which can assist in the understanding of these electrochemical tests.

Table 8 presents the quantity of some free metal ions (in ppm) in HW525 and HW540 (results from ICP-MS test). The difference of metal parts between these two fluids is not big as claimed by the fluid supplier. Figure 9 compares the chromatogram of HW525 and HW540 generated from GC-MS analysis. The overlap of each peak on the graph indicates that the organic additive packages in these two fluids are the same. Therefore, it can be suggested that the different glycol content causes the different behavior of nickel tungsten carbide in these two fluids.

With the higher glycol content (40%), HW540 is less corrosive than HW525 to nickel tungsten carbide. It is suggested that the glycol content inhibited the corrosion process by increasing the viscosity of the medium, which leads to a decrease in the diffusivity coefficient for the diffusion of the corrosion products out of the surface of the material (Ref 14).

Table 7 Comparison of the corrosion behavior of nickel tungsten carbide in four fluids at 50 °C

Fluid	HW540	HW525	HT	HT2
E_r, V	0.64	0.41	0.41	0.41
i_{corr}, μA/cm^2	1.29	1.74	3.55	3.02
OCP, V	−0.20	−0.18	−0.21	−0.22

Total results of ICP-MS analysis of the four fluids before and after the CPP tests are summarized in Table 9.

The most distinct finding from the above table is that a new free element Boron is detected after the test in HT and HT2, which is not observed on analysis of the fluid before the tests nor is it detected before and after the tests in HW525 and HW540.

From GC-MS analysis of HT and HT2 (Fig. 10 and 11), boratrane ($C_6H_{12}BNO_3$) that contains boron (full name: 2,8,9-trioxa-5-aza-1-borabicyclo[3.3.3]undecane) was explored while no component with boron exists in HW525 and HW540.

It is suggested that this organic compound would accept nickel from the material to form a new nickel boratrane compound and release free boron into the solution. Hence, it is a corrosive component to nickel tungsten carbide. This may be the main reason that nickel tungsten carbide behaves better in HW540 than in both HT and HT2.

Another interesting finding is that the Ni ion concentration after the tests is linear with the i_{corr} values, proving that Ni is a key element in the corrosion process.

However, the corrosion process is quite complex and it is hard to find out the exact mechanism and all the electrochemical reactions of this. Not all of the data in Table 6 can be explained at this moment.

Table 8 ICP-MS analysis results of HW525 and HW540 (in ppm)

	Al27	Cr52	Cu63	Fe56	K39	Mg24	Mn55	Na23	Zn66	Mo98
HW525	11	0.06	3	0.51	2	0	0.38	23	1	145
HW540	16	0.03	3	0.48	1	1	0.17	14	1	120

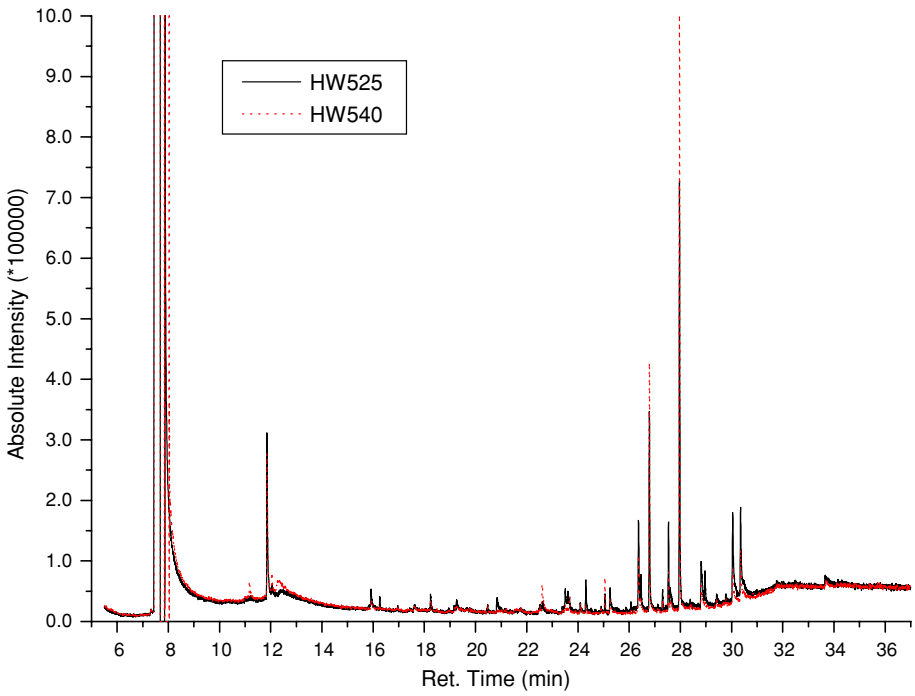

Fig. 9 The chromatogram of HW525 and HW540

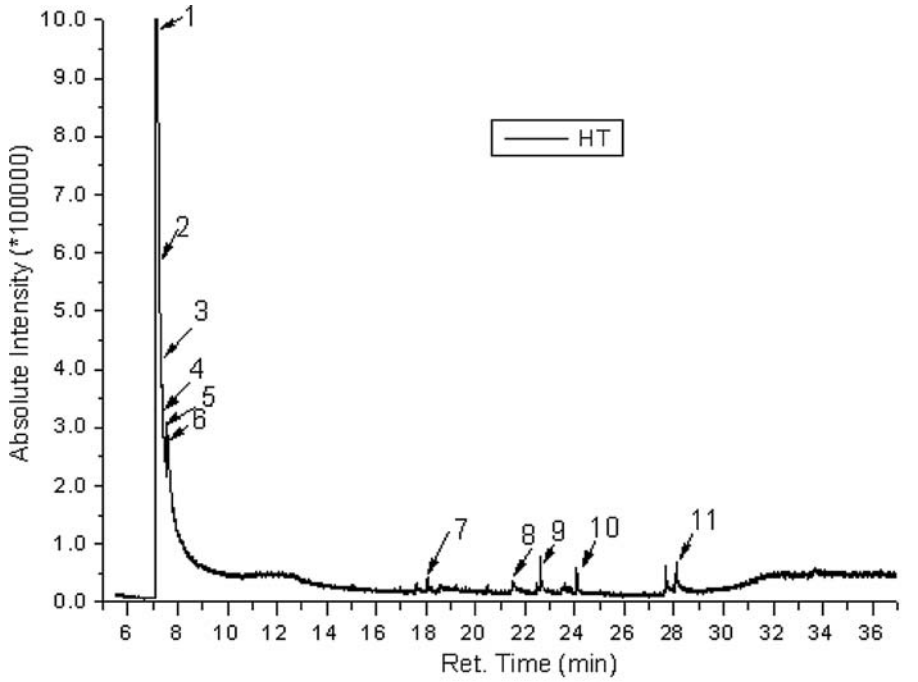

peak #	Ret.time (min)	Name	SI	CAS #	Mol. Weight	Mol.Form
8	21.49	2,8,9-Trioxa-5-aza-1-borabicyclo[3.3.3]undecane	90	283-56-7	157	$C_6H_{12}BNO_3$

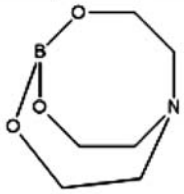

Fig. 10 Boratrane detected in HT by GC-MS

Table 9 ICP-MS analysis results of four fluids before and after CPP tests (in ppm)

	HW525		HW540		HT		HT2	
	Before test	After test	Before test	After test	Before test	After test	Before test	After test
Al27	11	10.40	16	14.70	2	0.12	1	0.20
Cr52	0.06	0.02	0.03	0.02	0.10	0.06	0.02	0.01
Cu63	3	3.76	3	3.68	1	1.84	0	0.30
Fe56	0.51	1.65	0.48	1.51	3.93	0.01	1.34	9.56
K39	2	0	1	0	12	13.6	3	0.09
Mg24	0	0.32	1	0.18	1	0.88	1	0.17
Mn55	0.38	0.16	0.17	0.06	1.97	0.86	0.24	0.12
Na23	23	18.60	14	9.48	309	0	653	0
Zn66	1	3.23	1	2.02	2	4.95	0	0.41
Mo98	145	0.17	120	0.18	0	0.85	0	0.03
B11	N/A	N/A	N/A	N/A	N/A	57.20	N/A	129
Ni60	N/A	0.09	N/A	0.05	N/A	0.59	N/A	0.16
W184	N/A	0.31	N/A	0.21	N/A	0.36	N/A	0.21

4. Conclusions

- Given that seawater ingress is hard to avoid in water depths greater than 150 m, nickel tungsten carbide may be a good alternative to stainless steel 316L since it is seawater tolerant as expected and performs better than stainless steel 316L at high temperature. However, it is an active material in these water-glycol hydraulic fluids and general corrosion occurs at a non-neglectable speed.
- Temperature increase and seawater ingress will accelerate the corrosion process of both nickel tungsten carbide and stainless steel 316L in each fluid, though the way may be different.

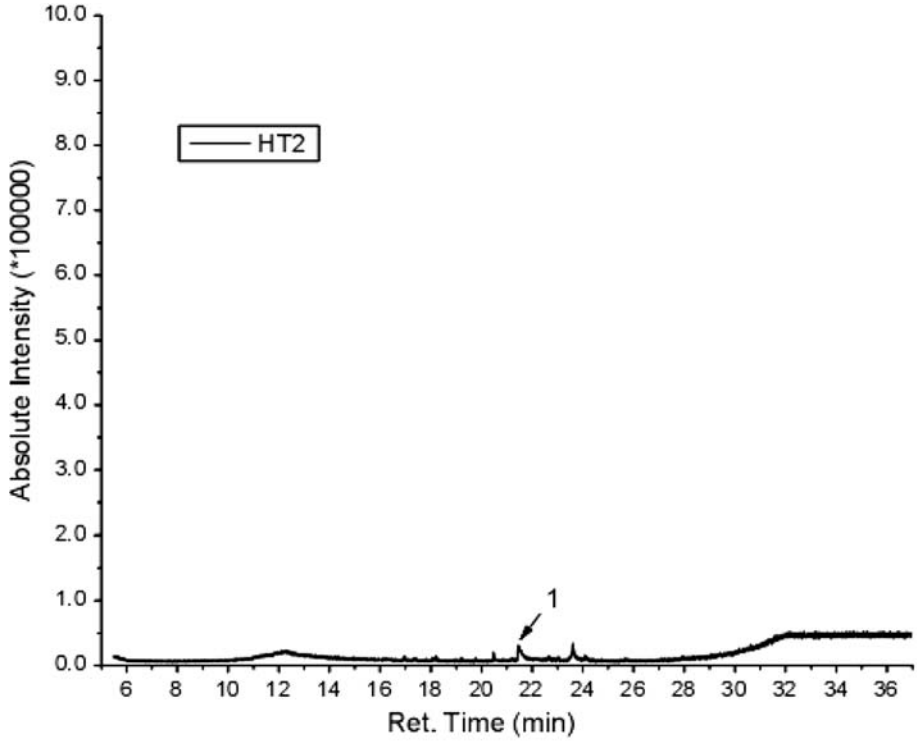

peak #	Ret.time (min)	Name	SI	CAS #	Mol. Weight	Mol.Form
1	21.46	2,8,9-Trioxa-5-aza-1-borabicyclo[3.3.3]undecane	89	283-56-7	157	$C_6H_{12}BNO_3$

Fig. 11 Boratrane detected in HT2 by GC-MS

- Fluid with high viscosity may be less corrosive to nickel tungsten carbide due to a reduction in corrosion product immigration from the surface.
- Boratrane found in HT and HT2 is presumed to be corrosive to nickel tungsten carbide.
- Summarizing all the CPP tests results, nickel tungsten carbide with fluid HW540 combination is the best choice.

Acknowledgment

This research work was sponsored by Aker-Kvaerner.

References

1. R. Fleming, BP Amoco Subsea Control System Lessons, *Meas. Control*, 2000, **33**(7), p 207–213
2. A.U. Malik, P.C. Mayan Kutty, N.A. Siddiqi, I.N. Andijani, and S. Ahmed, The Influence of pH and Chloride Concentration on the Corrosion Behaviour of AISI 316L Steel in Aqueous Solutions, *Corros. Sci.*, 1992, **33**(11), p 1809–1827
3. A.U. Malik, N.A. Siddiqi, and I.N. Andijani, Corrosion Behavior of Some Highly Alloyed Stainless Steels in Seawater, *Desalination*, 1994, **97**(1–3), p 189–197
4. K.S.E. Al-Malahy and T. Hodgkiess, Comparative Studies of the Seawater Corrosion Behaviour of a Range of Materials, *Desalination*, 2003, **158**(1–3), p 35–42
5. W.J. Tomlinson and C.R. Linzell, Anodic Polarization and Corrosion of Cemented Carbides with Cobalt and Nickel Binders, *J. Mater. Sci.*, 1988, **23**(3), p 914–918
6. K. Dasgupta, A. Chattapadhyay, and S.K. Mondal, Selection of Fire Resistant Hydraulic Fluids Through System Modeling and Simulation, *Simul. Modell. Pract. Theory*, 2005, **13**(1), p 1–20
7. U.S. Army Corps of Engineers, A144204, *Lubricants and Hydraulic Fluids*, p. 4-4 to 4-6
8. D. Reddy, Hydraulic Fluids, *Eng. Mater. Des.*, 1974, **18**(2), p 21–22
9. P.K.B. Hodges, *Hydraulic Fluids*, John Wiley & Sons, 1996, p 167
10. T.L. Sudesh, L. Wijesinghe, and D.J. Blackwood, Characterisation of Passive Films on 300 Series Stainless Steels, *Appl. Surf. Sci.*, 2006, **253**(2), p 1006–1009
11. A. Neville, T. Hodgkiess, and X. Destriau, Initiation and Propagation of Localised Corrosion on Stainless Steels in Seawater Containing High Biocide Concentrations, *Corros. Sci.*, 1998, **40**(4–5), p 715–730
12. J. Stewart and D.E. Williams, The Initiation of Pitting Corrosion on Austenitic Stainless Steel: On the Role and Importance of Sulphide Inclusions, *Corros. Sci.*, 1992, **33**(3), p 457–474
13. G. Wranglen, Pitting and Sulphide Inclusions in Steel, *Corros. Sci.*, 1974, **14**(5), p 331–349
14. B.A. Abd-El-Nabey, N. Khalil, M.M. Eisa, and H. Sadek, Pitting Corrosion of Stainless Steel in Water-Organic Solvent Mixtures, *Surf. Technol.*, 1983, **20**(3), p 209–217